iScience

CellPress
OPEN ACCESS

Article

Therapeutic exosomal vaccine for enhanced cancer immunotherapy by mediating tumor microenvironment

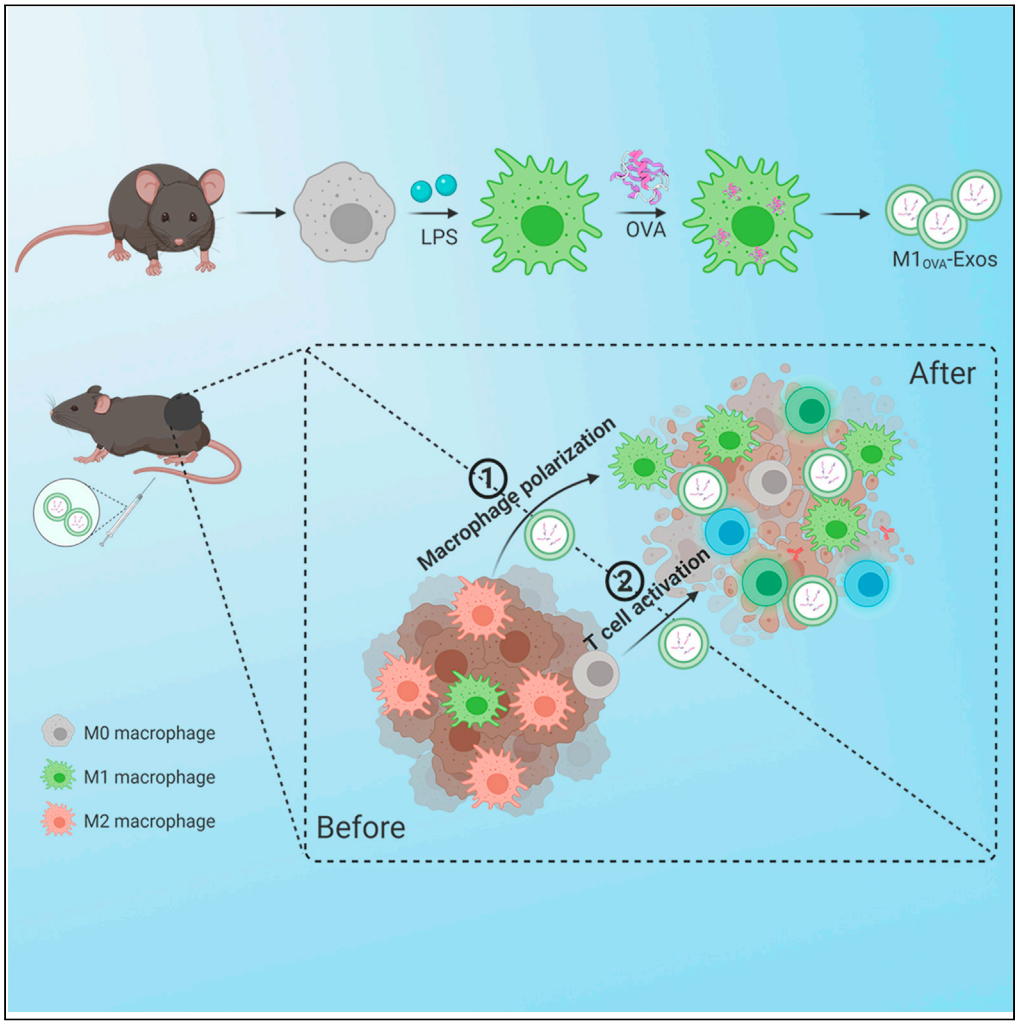

Fangfang Lv, Huifang Liu, Gaoqian Zhao, ..., Jinchao Zhang, Xing-Jie Liang, Zhenhua Li

liu-huifang@163.com (H.L.)
liangxj@nanoctr.cn (X.-J.L.)
zhenhuali@hbu.edu.cn (Z.L.)

Highlights

$M1_{OVA}$-Exos polarizes TAMs into M1 type by downregulates Wnt signaling

$M1_{OVA}$-Exos effectively inhibits tumor growth and metastasis

$M1_{OVA}$-Exos enhanced vaccine-based immunotherapy by mediating the TME

Lv et al., iScience 25, 103639
January 21, 2022
https://doi.org/10.1016/j.isci.2021.103639

iScience

CellPress
OPEN ACCESS

Article

Therapeutic exosomal vaccine for enhanced cancer immunotherapy by mediating tumor microenvironment

Fangfang Lv,[1,3,6] Huifang Liu,[1,3,6,*] Gaoqian Zhao,[1,3,6] Erman Zhao,[1,3] Hongyu Yan,[3,4] Ruijun Che,[3,4] Xinjian Yang,[3,4] Xiaohan Zhou,[2] Jinchao Zhang,[3,4] Xing-Jie Liang,[5,7,*] and Zhenhua Li[2,*]

SUMMARY

Tumor immunotherapy has been convincingly demonstrated as a feasible approach for treating cancers. Although promising, the immunosuppressive tumor microenvironment (TME) has been recognized as a major obstacle in tumor immunotherapy. It is highly desirable to release an immunosuppressive "brake" for improving cancer immunotherapy. Among tumor-infiltrated immune cells, tumor-associated macrophages (TAMs) play an important role in the growth, invasion, and metastasis of tumors. The polarization of TAMs (M2) into the M1 type can alleviate the immunosuppression of the TME and enhance the effect of immunotherapy. Inspired by this, we constructed a therapeutic exosomal vaccine from antigen-stimulated M1-type macrophages ($M1_{OVA}$-Exos). $M1_{OVA}$-Exos are capable of polarizing TAMs into M1 type through downregulation of the Wnt signaling pathway. Mediating the TME further activates the immune response and inhibits tumor growth and metastasis via the exosomal vaccine. Our study provides a new strategy for the polarization of TAMs, which augments cancer vaccine therapy efficacy.

INTRODUCTION

The tumor microenvironment (TME) refers to the interaction between tumor cells and their surrounding tissue components, all of which form a complex internal environment that is conducive to the biological behavior of tumor cells (Gao et al., 2019; Zhang et al., 2019). TME consists of a heterogeneous population, including cancer cells, infiltrating immune cells, and stromal cells (Hanahan and Weinberg, 2011; Lei et al., 2020). There are a large number of immune cells that promote tumor development in the TME. Regulatory cells (Tregs), myeloid-derived suppressor cells (MDSCs), and tumor-associated macrophages (TAMs) are the most important components (Zhang et al., 2019; Davis et al., 2016). The TME is mostly immunosuppressive, and thereby greatly affecting the effects of immunotherapy.

Macrophages account for a large proportion (about 50%) of the TME (Vitale et al., 2019; Lopez-Yrigoyen et al., 2020; Goldman et al., 2017). They are the main component of immunosuppressive cells and play an important role in immunosuppression. Macrophages have two main distinct phenotypes. M1 macrophages promote antitumor functionality via enhancing antigen presentation and Th1 activation, as well as by secreting pro-inflammatory cytokines. In contrast, M2 macrophages promote tumor invasion, growth, and metastasis by secreting immunosuppressive cytokines and chemokines to suppress immunity (Yang et al., 2020; Singh et al., 2017). In TAMs, macrophages mostly exhibit the functionality of the M2 type. Polarizing TAMs to the M1 type can effectively reverse tumor immunosuppression, which then improves the efficiency of T cell activation and significantly enhances the effect of tumor immunotherapy. Macrophages have a high plasticity (Locati et al., 2019; Guilliams and Svedberg, 2021), which provides a basis for mediating the tumor immunosuppressive microenvironment by domesticating TAMs into M1-like macrophages. For example, Wang et al. used IL-12-loaded and microenvironment-responsive nanoparticles to reeducate TAMs for enhanced tumor immunotherapy (Wang et al., 2017). Weissleder et al. used R848-loaded cyclodextrin nanoparticles to effectively deliver the TLR7/8 agonist R848 to TAMs *in vivo* to polarize them into M1 phenotype (Rodell et al., 2018), thereby controlling tumor growth and protecting animals from tumor invasion. These nanocarriers, however, are mainly exogenous materials that entail high immunogenicity and potential biosafety issues. Endogenous materials such as exosomes (Exos) have been widely used

[1]College of Pharmaceutical Science, Key Laboratory of Pharmaceutical Quality Control of Hebei Province, Institute of Life Science and Green Development, Hebei University, Baoding 071002, China

[2]Affiliated Dongguan Hospital, Southern Medical University, Dongguan 523059, China

[3]Key Laboratory of Medicinal Chemistry and Molecular Diagnosis of Ministry of Education, Chemical Biology Key Laboratory of Hebei Province, Hebei University, Baoding 071002, China

[4]College of Chemistry & Environmental Science, Institute of Life Science and Green Development, Hebei University, Baoding 071002, China

[5]CAS Key Laboratory for Biological Effects of Nanomaterials and Nanosafety National Center for Nanoscience and Technology, Beijing 100190, China

[6]These authors contributed equally

[7]Lead contact

*Correspondence: liu-huifang@163.com (H.L.), liangxj@nanoctr.cn (X.-J.L.), zhenhuali@hbu.edu.cn (Z.L.)

https://doi.org/10.1016/j.isci.2021.103639

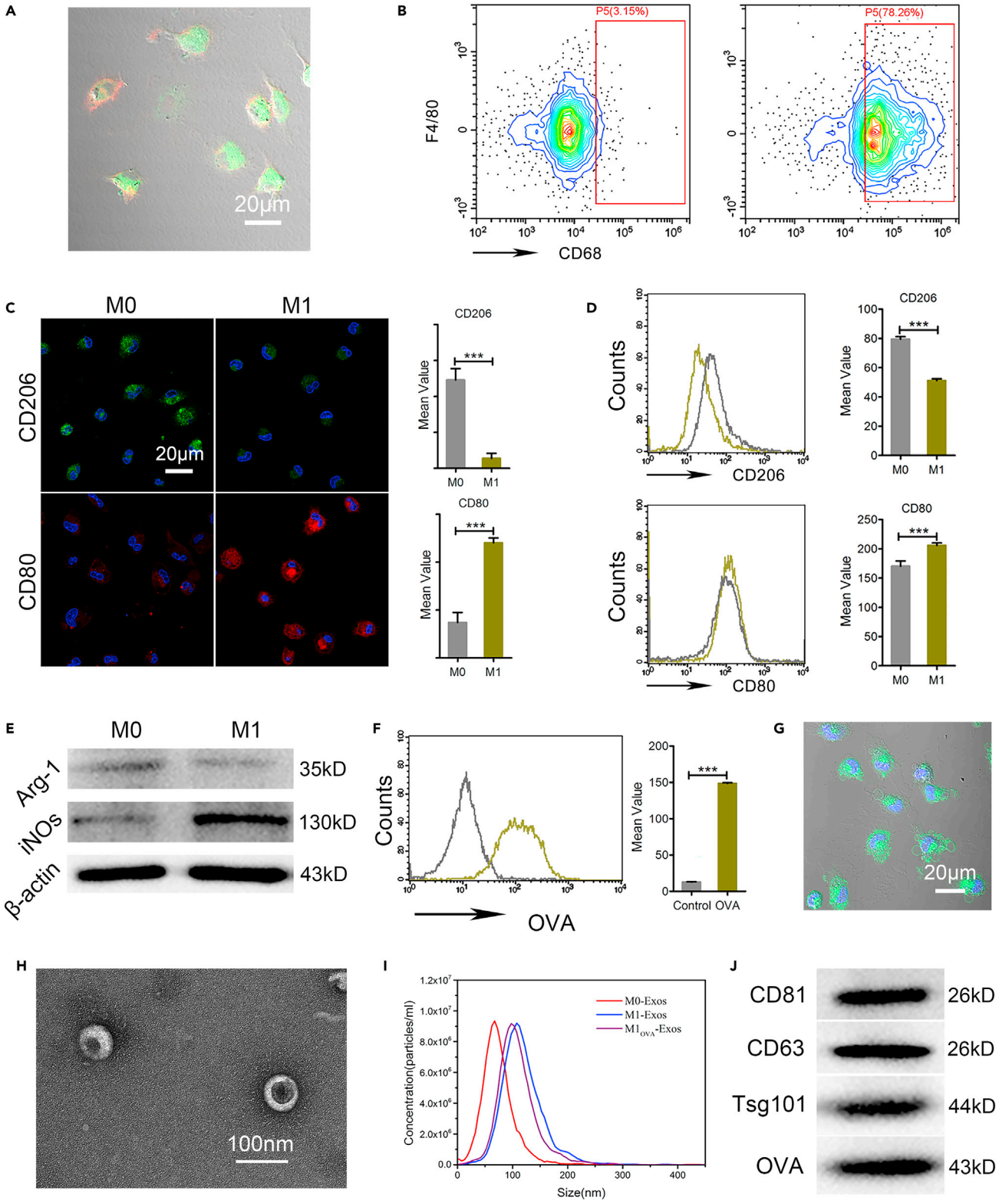

Figure 1. Construction and characterization of $M1_{OVA}$-Exos

(A and B) The expression of F4/80 and CD68 in primary macrophages was analyzed by CLSM (A) and FCM (B).

(C and D) Macrophages were polarized by LPS; the expression of CD206 and CD80 before and after polarization was analyzed by CLSM (C) and FCM (D). n = 3.

Figure 1. *Continued*
(E) The expression of Arg-1 and iNOs was analyzed by WB.
(F and G) Macrophages internalized OVA-FITC. FCM (F) and CLSM (G) were used to verify the uptake of OVA by macrophages. n = 3.
(H) TEM image of $M1_{OVA}$-Exos.
(I) The NTA analysis of M0-Exos, M1-Exos, and $M1_{OVA}$-Exos.
(J) The WB analysis of exosomal markers. All statistical data are represented as mean ± SD and Student-Newman-Keuls Multiple Comparisons Test was done for statistical analyses. ***$p < 0.001$.

as carriers for therapeutic agents (Li et al., 2016, 2019; Ke and Afonin, 2021; Liu and Su, 2019). Exos are derived from the collapse of intracellular lysosomes to form multivesicular bodies, which are nanovesicles with a diameter of 30-150nm (Pegtel and Gould, 2019; Kalluri and Lebleu, 2020). Exos contain complex RNA and proteins of the parent cells (Pegtel and Gould, 2019; Kalluri and Lebleu, 2020; Kalluri, 2016; Jeppesen et al., 2019). Based on this, the Exos from M1 macrophages (M1-Exos) have been proved to polarize macrophages into M1 phenotype (Nie et al., 2020; Wang et al., 2019). Therefore, M1-Exos were used to polarize TAMs and improve the TME. Furthermore, we first used OVA, a widely used model antigen in preclinical studies (Leick et al., 2019; Xu et al., 2019), to stimulate M1 macrophages, and then isolated Exos from them. Thus, OVA/OVA-antigen peptides would be present on the Exos to give an exosomal vaccine ($M1_{OVA}$-Exos).

Our $M1_{OVA}$-Exos can be regarded as a therapeutic tumor vaccine capable of polarizing M2 macrophages to M1 therapeutic phenotype. Our $M1_{OVA}$-Exos with good biocompatibility and long circulating time indicates a very promising therapeutic tumor vaccine (Trams et al., 1981; Colombo et al., 2014; Zhu et al., 2020).

RESULTS

Characterization of primary macrophages

Primary macrophages were obtained through the abdominal cavity lavage experiment and characterized by ink phagocytosis experiments. The morphology of primary macrophages was shown in Figure S1A with complete morphology and good condition. Then, our ink phagocytosis experiments verified the phagocytosis ability of primary macrophages (Figure S1B). CD68 and F4/80 were two characteristic markers for macrophages and CLSM and FCM were used to analyze these specific markers of macrophages. As shown in Figures 1A and 1B, the results showed that the extracted primary macrophages positively expressed CD68 and F4/80, proving that the extracted primary cells were indeed macrophages.

Macrophages polarization by lipopolysaccharide (LPS)

To obtain M1-like macrophages, we stimulated primary macrophages (M0 phenotype) with LPS at a concentration of 100 ng/mL. We compared the macrophage phenotypes before and after LPS polarization. CD206 and CD80 were commonly used biomarkers of M2 macrophages and M1 macrophages, respectively. As shown in Figure 1C, the results of CLSM showed that the level of CD80 (red fluorescence) on the macrophage surface after polarization by LPS was significantly increased compared with that of before polarization. In contrast, the expression of CD206 (green fluorescence) was significantly reduced. The results of FCM (Figure 1D) were consistent with those of CLSM that LPS stimulated macrophages toward M1 phenotype. In addition, we used Western blot (WB) analysis to detect the expression level of iNOs and Arg-1. The results showed that iNOs expression increased and Arg-1 expression decreased after LPS polarization (Figure 1E). Taken together, these results proved that LPS successfully polarized primary macrophages into M1 macrophages.

M1 macrophages showed stronger phagocytic ability. Subsequently, we incubated OVA with M1 macrophages to induce antigen-presentation. FITC-labeled OVA antigen (FITC-OVA) was synthesized and used to study the internalization of OVA by macrophages. After 24 h of incubation with M1 macrophages, the colocalization of OVA antigen with macrophages was investigated by CLSM and FCM. As shown in Figures 1F and 1G, OVA (green fluorescence) was found within macrophages, indicating that the macrophages had effectively internalized OVA antigens.

The extraction and characterization of $M1_{OVA}$-Exos

Exos are metabolites created during the ordinary life activities of cells. After obtaining OVA antigen-stimulated M1 macrophages, we isolated the Exos ($M1_{OVA}$-Exos) from the cell culture supernatant through an experimental method combining ultrafiltration and ultracentrifugation. To confirm the physical and

chemical properties of $M1_{OVA}$-Exos, we first used TEM to characterize their morphology and size. As shown in Figure 1H, $M1_{OVA}$-Exos were spherical with uniform size. Subsequently, we used DLS to characterize the zeta potential of M0-Exos, M1-Exos, and $M1_{OVA}$-Exos. As shown in Figure S2, the zeta potentials of M0-Exos, M1-Exos, and $M1_{OVA}$-Exos were −17.41 mV, −16.80 mV, and −22.95 mV, respectively. In addition, as shown in Figure 1I, the particle size and concentration of M0-Exos, M1-Exos, and $M1_{OVA}$-Exos were calculated by NanoSight. TSG101, CD9, CD63, and CD81 are commonly used makers for all kinds of Exos. As shown in Figure S3, the FCM results indicated that the $M1_{OVA}$-Exos highly expressed CD63 and CD81. The WB results also showed that $M1_{OVA}$-Exos exhibited a high expression of CD63, CD81, and Tsg101, which was consistent with these FCM results (Figure 1J). Furthermore, OVA antigens were detected from the extracted Exos as well (Figure 1J).

Macrophages efficiently internalize $M1_{OVA}$-Exos

$M1_{OVA}$-Exos were designed to polarize macrophages and their interaction was then investigated. As shown in Figure 2A, the CLSM images showed that both RAW264.7 and B16-OVA could internalize DiO-labeled $M1_{OVA}$-Exos, whereas RAW264.7 have a stronger binding ability to $M1_{OVA}$-Exos. The FCM results further confirmed that RAW264.7 had a stronger ability to internalize $M1_{OVA}$-Exos compared with B16-OVA (Figure 2B).

$M1_{OVA}$-Exos polarize macrophages and stimulate immune response

Exos carry RNA and protein components of the parent cell and are involved in signal transduction. To evaluate whether M1-Exos can polarize macrophages into M1 phenotype, CLSM, and FCM were used to observe the biomarkers of M1-macrophages. As shown in Figures 2C and S4, the results showed that both M1-Exos and $M1_{OVA}$-Exos can increase the expression of CD80 of RAW264.7 and decrease the expression of CD206, which indicated that M1-Exos and $M1_{OVA}$-Exos can effectively polarize macrophages to the M1 phenotype.

Macrophages can secrete cytokines to affect tumor immunotherapy. In addition, macrophages are also antigen-presenting cells (APCs) that participate in tumor immunotherapy. M1-Exos and $M1_{OVA}$-Exos not only polarized macrophages into the M1 type but also enhanced the antigen presentation ability. We used FCM to analyze the effects of PBS, OVA, M0-Exos, M1-Exos, and $M1_{OVA}$-Exos on macrophages' antigen presenting ability. As shown in Figure 2D, the results showed that the fluorescence intensity of SIINFEKL/PE in M1-Exos and $M1_{OVA}$-Exos treated groups were significantly stronger than that of the PBS group. Our results indicated that M1-Exos and $M1_{OVA}$-Exos could not only polarize macrophages into M1 phenotype but also enhance the antigen presenting ability.

The activation of T cells plays a vital role in immunotherapy. The following verified that OVA antigen included M1-Exos could activate T cells *in vitro*. PBS, OVA, M0-Exos, M1-Exos, and $M1_{OVA}$-Exos were incubated with Jurkat (clone E6-1) cells, and cells were collected by centrifugation and stained with CD4/PE or CD8a/PE for FCM analysis. As shown in Figure 2E, CD4 and CD8 positive Jurkat (clone E6-1) cells were detected in the $M1_{OVA}$-Exos treated group. *In vitro* T cell activation experiments showed that $M1_{OVA}$-Exos could effectively activate T cells into $CD4^+$ T cells and $CD8^+$ T cells.

Mechanism of M1-Exos polarizing macrophages

We next studied the mechanism of M1-Exos polarizing macrophages into M1 macrophages by RNA sequence. As shown in Figure 2F, compared with M0-Exos, M1-Exos upregulated some strands of miRNA related to the polarization of M1 macrophages such as miR-101, miR-125, miR-155, and miR-21. In addition, let-7c and let-7f were downregulated which were related to the polarization of M2 macrophages.

Next, we performed KEGG signaling pathway analysis on the target genes of the differential miRNA obtained by sequencing. As shown in Figure 2G, KEGG analysis showed that the polarization of macrophages toward M1 phenotype by M1-Exos was related to the Wnt signaling pathway. It has been reported that the inhibition of M2-like TAMs and Wnt/β-catenin signaling pathway could inhibit tumor growth, metastasis, and facilitate the polarization of macrophages toward the M1 phenotype (Sha et al., 2017; Lv et al., 2020). For this reason, we verified whether M1-Exos promote the polarization of macrophages to M1 phenotype by inhibiting the Wnt signaling pathway. As shown in Figure 2H, the expression of some key proteins (β-Catenin, c-Myc, and Cyclin D1) in the Wnt signaling pathway decreased after treatment with M1-Exos. The results of CLSM also showed that the fluorescence of β-catenin in macrophages decreased after

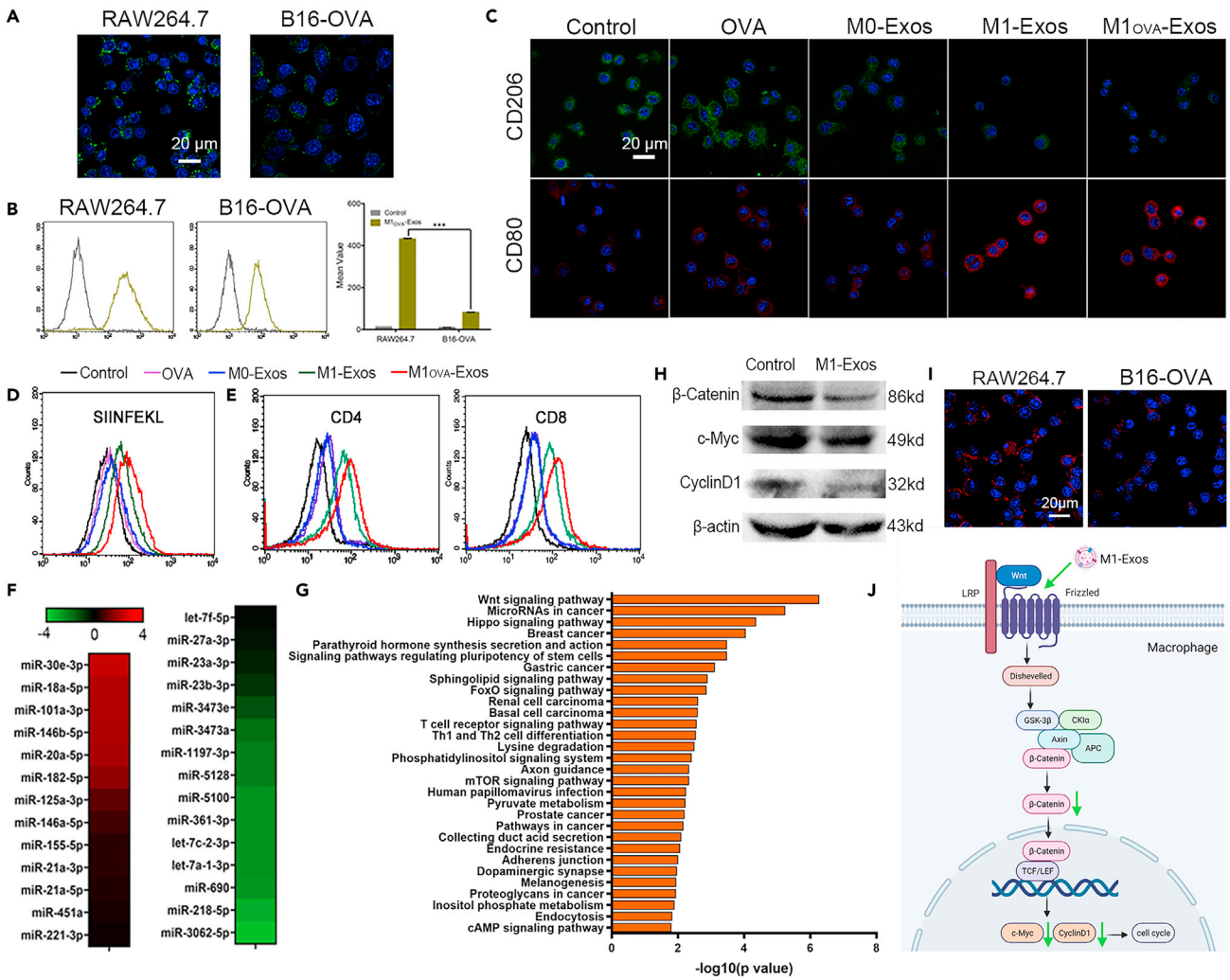

Figure 2. The effect and mechanism of $M1_{OVA}$-Exos *in vitro*

(A and B) CLSM (A) and FCM (B) analysis of $M1_{OVA}$-Exos internalization rate by RAW264.7 and B16-OVA cells. n = 3.

(C) CLSM images showed the expression of CD80 and CD206 after treatment.

(D) Evaluate the expression of SIINFEKL by FCM after being treated with PBS, OVA, M0-Exos, M1-Exos, and $M1_{OVA}$-Exos.

(E) $CD4^+$ T cells and $CD8^+$ T cells activation after treatment.

(F) miRNA sequencing for M0-Exos and M1-Exos. Red and green bars indicated miRNA expressions were upregulated and downregulated when compared with M0-Exos.

(G) KEGG signaling pathway analysis for miRNA targeting genes.

(H) The effect of M1-Exos treatment on the expression of β-Catenin, Cyclin D1, and c-Myc in RAW264.7.

(I) Fluorescence of β-Catenin in RAW264.7 before and after M1-Exos treatment.

(J) Wnt signal pathway diagram. All statistical data are represented as mean ± SD and Student-Newman-Keuls Multiple Comparisons Test was done for statistical analyses. ***$p < 0.001$.

treatment with M1-Exos (Figure 2I). These results together indicated that M1-Exos could inhibit the Wnt signaling pathway (Figure 2J). Therefore, the ability of M1-Exos to polarize macrophages into M1 type was mainly attributed to the downregulation of the Wnt signaling pathway.

$M1_{OVA}$-Exos inhibit tumor growth *in vivo*

To verify whether the combined therapy of TAMs polarization to regulate the TME and an OVA-specific tumor vaccine could enhance the growth inhibition of tumors, PBS, OVA, M0-Exos, M1-Exos, and $M1_{OVA}$-Exos were administered to B16-OVA tumor–bearing mice *via* tail vein injection. The tumor size of each group was measured every two days. As shown in Figures 3C–3E, the tumors grew rapidly when treated

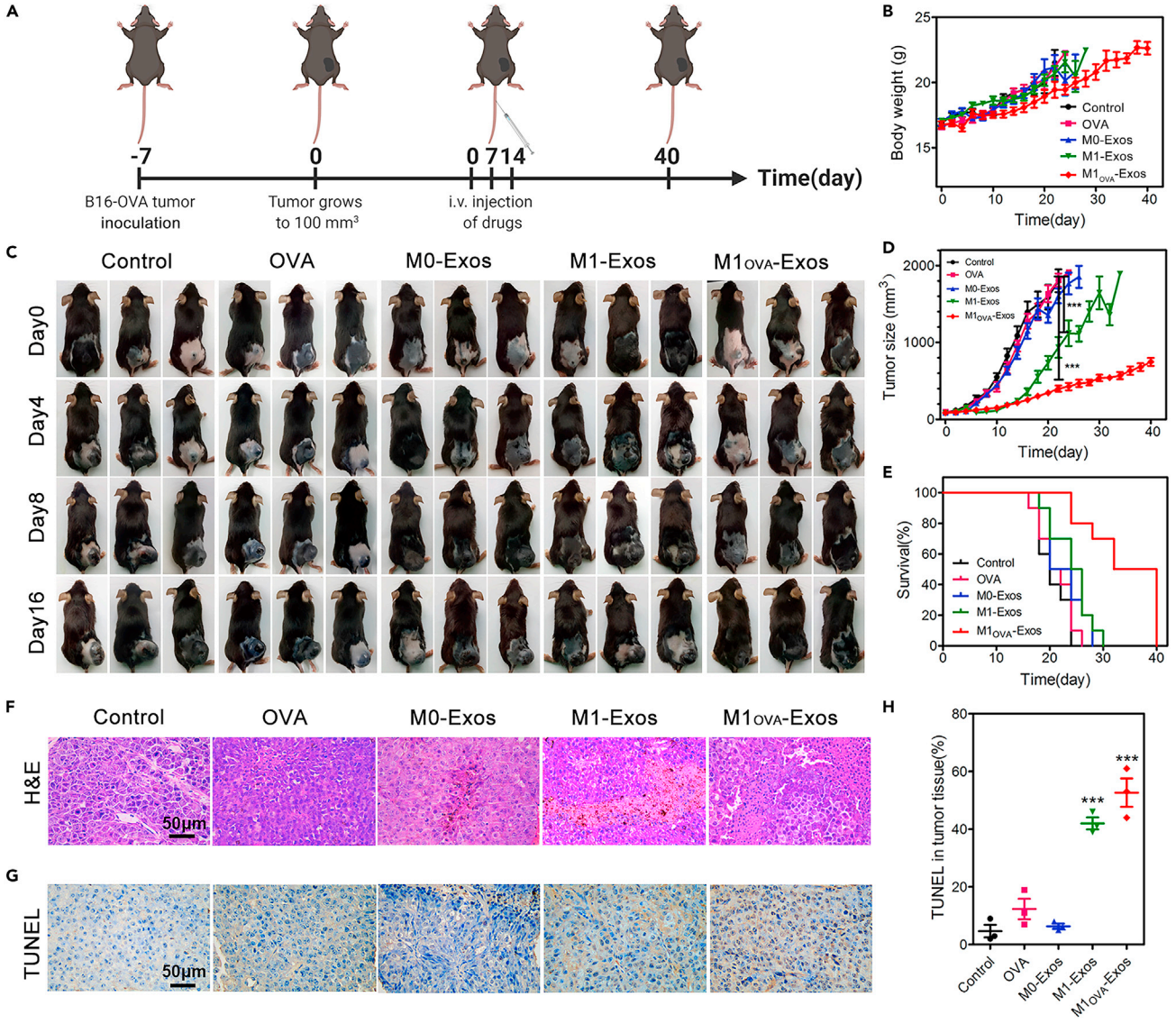

Figure 3. Study of therapeutic effect of $M1_{OVA}$-Exos on B16-OVA tumor-bearing mice

(A) Schematic illustrating the animal work plan of B16-OVA tumor-bearing mice.

(B) Changes in body weight of five groups during treatment.

(C) Representative photographs of tumor volume changes during treatment.

(D) Tumor volume assessment at the therapeutic period.

(E) Survival rate of B16-OVA tumor-bearing mice in the therapy model.

(F) H&E staining of the dissected tumors after treatments.

(G) TUNEL analysis of tumor cell apoptosis.

(H) Quantitative TUNEL-positive cells. All statistical data are represented as mean ± SD (n = 3), and Student-Newman-Keuls Multiple Comparisons Test was done for statistical analyses. ***$p < 0.001$, compared with control.

with PBS, OVA, and M0-Exos. In the M1-Exos treated group, the tumors were not completely suppressed, indicating that the polarization of TAMs to the M1 phenotype only had a certain inhibitory effect on tumor growth. In contrast, even after 40 days treatment, the tumor volume growing rate in the $M1_{OVA}$-Exos treated group remained slower, showing obvious anti-tumor effects. More importantly, $M1_{OVA}$-Exos significantly prolonged the survival time of tumor-bearing mice as well, with 5 mice still surviving at the end of the 40-day experiment. During the entire experiment, we also monitored the weight change of mice. As shown in Figure 3B, there was basically no difference in their body weight, demonstrating that the injected materials have a slight effect on the weight change of the mice.

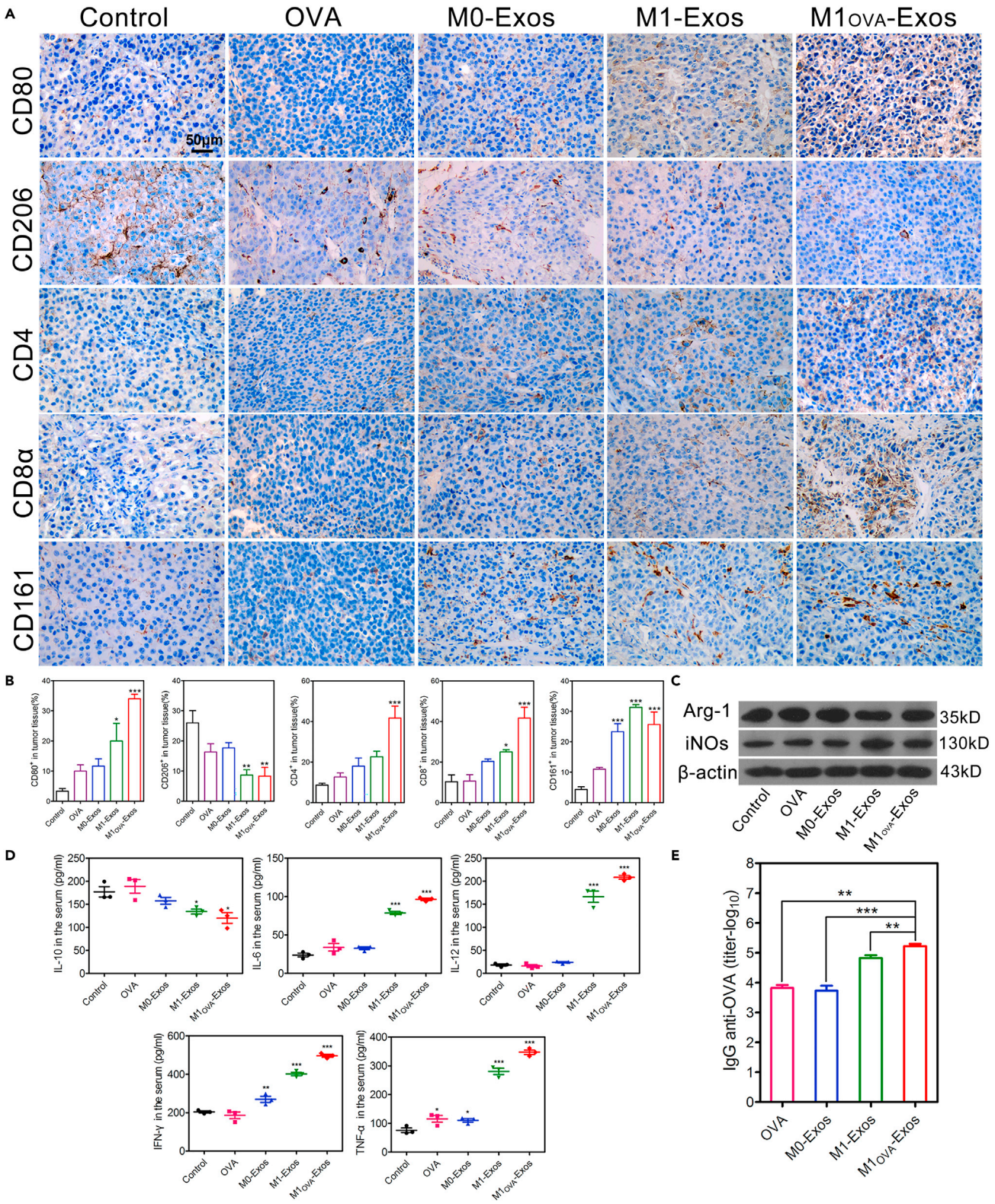

Figure 4. Immune activation of $M1_{OVA}$-Exos on B16-OVA tumor-bearing mice

(A) IHC analysis of the expression of CD80, CD206, CD4, CD8, and CD161 in the tumor tissues of tumor-bearing mice after treatment.

(B) Statistics of positive cells from IHC data.

Figure 4. *Continued*

(C) The expression of Arg-1 and iNOs in the tumor tissues analyzed by WB.

(D) ELISA analysis of the serum cytokine content in different treatment groups.

(E) Determination of OVA antibody titers in the serum of tumor-bearing mice. All statistical data are represented as mean ± SD (n = 3), and Student-Newman-Keuls Multiple Comparisons Test was done for statistical analysis. *p < *0.05*, **p < *0.01*, ***p < *0.001*, compared with the indicated groups or with the control.

H&E staining was used to conduct pathological analyses on the hearts, livers, spleens, lungs, kidneys, and tumors of the different groups to evaluate the materials' biological safety and the killing effect on tumor tissues. H&E staining results showed no obvious damage to main organs in each group (Figure S5), indicating that $M1_{OVA}$-Exos had no apparent toxicity. The tumor cells treated with $M1_{OVA}$-Exos showed obvious nuclear shrinkage, blurred cell boundaries, and the disappearance of cell morphology, demonstrating tumor cells underwent obvious necrosis (Figure 3F). As shown in Figures 3G and 3H, TUNEL staining results of the $M1_{OVA}$-Exos treatment group exhibited a clear positive reaction, indicating that the level of apoptosis in the tumor tissue was higher and the growth of tumors was significantly inhibited. This result was consistent with the results obtained by H&E. Experiments at the animal level showed that $M1_{OVA}$-Exos could effectively inhibit tumor growth and improve the body survival rate.

The effect of $M1_{OVA}$-Exos on immunoregulation

An important reason why $M1_{OVA}$-Exos can effectively inhibit tumor growth and prolong the survival time of tumor-bearing mice was the polarization of TAMs into M1 macrophages. M1-type macrophages can directly kill tumors. In addition, M1 macrophages can also reduce the immunosuppressive effect of the TME and enhance tumor immunotherapy. We used FCM, IHC, WB, and other methods to analyze the phenotype of tumor-infiltrating macrophages in different groups. CD80 is highly expressed on the surface of M1 macrophages, whereas CD206 is highly expressed on the surface of M2 macrophages. As shown in Figures 4A and 4B and Figure S6, IHC and FCM showed that more M1 macrophages infiltrated the tumor tissue in the $M1_{OVA}$-Exos treated group. As shown in Figure 4C, WB results showed that the M1 macrophage-related protein iNOS was elevated in tumor tissues treated by $M1_{OVA}$-Exos, whereas the M2 macrophage-related protein Arg-1 had decreased.

Different phenotypes of macrophages secrete different cytokines to play their roles: M1 macrophages mainly secrete pro-inflammatory cytokines such as IL-6, IL-12, TNF-α, and IFN-γ to enhance immunotherapywhile M2 macrophages mainly secrete anti-inflammatory cytokines, such as IL-10. We measured the levels of IL10, IL-6, IL-12, TNF-α, and IFN-γ in the serum via ELISA (Figure 4D). The content of IL-10 in M1-Exos and $M1_{OVA}$-Exos was reduced to a certain extent. The levels of IL-6, IL-12, TNF-α, and IFN-γ increased significantly in the M1-Exos and $M1_{OVA}$-Exos group. Moreover, the $M1_{OVA}$-Exos group had a higher level than that of M1-Exos, which may be related to the stronger activation of T cells by $M1_{OVA}$-Exos as a tumor vaccine. By measuring the titer of OVA antibody in serum of tumor-bearing mice (Figure 4E), the mice of $M1_{OVA}$-Exos group could specifically produce more OVA antibodies, which was statistically significant compared with OVA group and M1-Exos group.

To detect T cell proliferation and activation in tumor tissues of different groups, we collected fresh tumor tissues for FCM analysis (Figure S7). Compared with the other groups, the infiltration of $CD4^+$ T cells and $CD8^+$ T cells in the $M1_{OVA}$-Exos treated group was significantly higher, which showed that $M1_{OVA}$-Exos as a tumor vaccine promoted the proliferation and activation of T cells. Thus, the infiltration of immune cells would promote the "cold" tumor changing to "hot" tumor. In addition, the increase of T cells was attributed to the polarization of TAMs into M1 macrophages by M1-Exos, which alleviated the immunosuppression of the TME. As shown in Figures 4A and 4B, the IHC analysis showed that the $M1_{OVA}$-Exos group had a higher number of $CD4^+$ T cells and $CD8^+$ T cells in the tumor tissues compared with the control group, which is consistent with the results of FCM. Likewise, the $M1_{OVA}$-Exos treatment group also had more NK cell infiltration. In addition, the results of the positive cell count in the IHC analysis also showed that $M1_{OVA}$-Exos activated the immune system and significantly promoted the immune-cell infiltration of tumors, turning it into a "hot" tumor.

$M1_{OVA}$-Exos inhibit metastasis *in vivo*

Lung metastasis often accompanies the development of malignant tumors. To explore whether $M1_{OVA}$-Exos can effectively inhibit tumor metastasis while inhibiting tumor growth, we constructed a lung metastasis model. After treatment, we collected representative metastatic lung tissues and calculated the

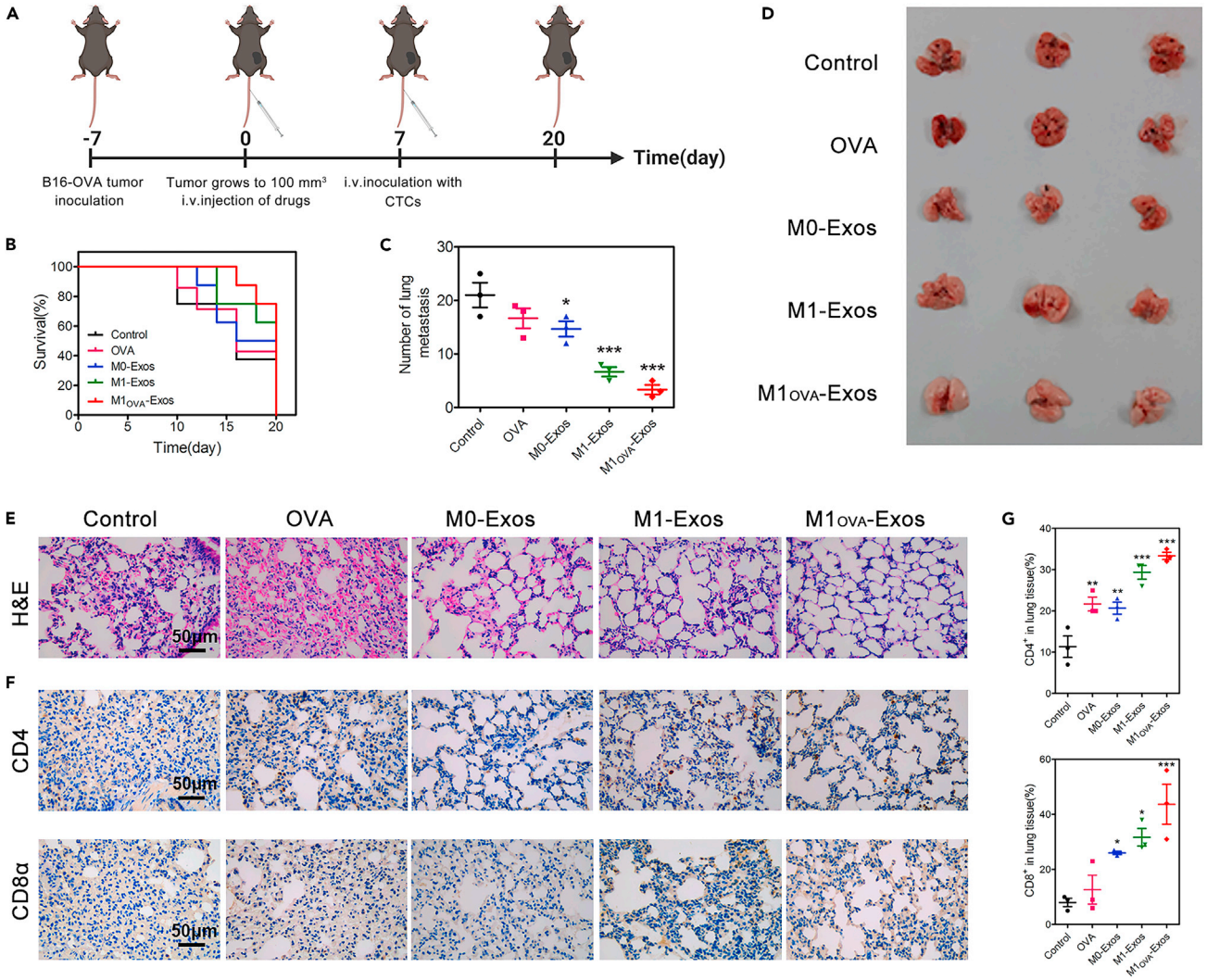

Figure 5. The inhibitory effect of $M1_{OVA}$-Exos on lung metastasis of B16-OVA tumor

(A) Schematic illustrating the design of B16-OVA lung metastasis model.

(B) Survival rate of metastasis mice.

(C) The number of lung nodules in different treatment groups.

(D) Lung images of different groups.

(E) H&E staining of lung tissue.

(F) IHC analysis of the infiltration of $CD4^+$ T cells and $CD8^+$ T cells in lung tissues.

(G) Statistics of positive cells from IHC data. All statistical data are represented as mean ± SD (n = 3), and Student-Newman-Keuls Multiple Comparisons Test was done for statistical analysis. *p < *0.05*, **p < *0.01*, ***p < *0.001*, compared with control.

number of lung nodules in each group. It was found that the control group had obvious metastasis, whereas the $M1_{OVA}$-Exos treatment group had a significant reduction in the average number of lung metastases, presenting a significant difference from the control group (Figures 5C and 5D). In addition, as shown in Figure 5B, compared with the control group, the survival rate of mice in the treatment group was significantly improved. We performed H&E staining on the lung metastasis tissue of tumor-bearing mice, and the results of pathological analysis also proved that the lung injuries sustained by the mice in the $M1_{OVA}$-Exos treatment group were significantly reduced (Figure 5E). These results all indicated that $M1_{OVA}$-Exos can effectively inhibit lung metastasis. IHC analysis was performed on the lung tissue of the metastasis model (Figures 5F and 5G). The results showed that after $M1_{OVA}$-Exos treatment, the infiltration of $CD4^+$ T cells and $CD8^+$ T cells in the lung was significantly increased, indicating that $M1_{OVA}$-Exos treatment could effectively prevent lung metastasis.

DISCUSSION

In recent years, although immunotherapy has made great progress in the treatment of tumors, the immunosuppressive tumor microenvironment formed during the development of tumors has severely restricted the therapeutic efficiency of immunotherapy (Couzin-Frankel, 2013; Yang et al., 2020). Macrophages are the most abundant immune cells in the TME (Fang et al., 2018). The different phenotypes of macrophages play a completely different role in the occurrence and development of tumors. Therefore, reeducation of TAM can regulate the immune status of the TME and enhance the effect of immunotherapy (Cheng et al., 2017; Chen et al., 2018; Zanganeh et al., 2016; Lan et al., 2019).

In our study, the exosomes of M1 macrophages were selected to regulate the TME and enhance the immunotherapy effect of $M1_{OVA}$-Exos on B16-OVA melanoma. As shown in Figure 1, the primary macrophages were successfully polarized into M1 macrophages by LPS, and after ingesting OVA antigen, their exosomes ($M1_{OVA}$-Exos) were isolated as tumor vaccines that can improve tumor immune microenvironment for efficiently antitumor immunotherapy.

Our $M1_{OVA}$-Exos can polarize macrophages to M1 type and enhance the antigen presentation ability of macrophages to activate immune response. To clarify the mechanism of M1-Exos polarizing macrophages, the miRNAs of M0-Exos and M1-Exos were sequenced and analyzed, and the results were shown in Figure 2F. Compared with M0-Exos, the expression of miRNAs (miR-101, miR-125, miR-155, and miR-21) associated with M1 macrophages in M1-Exos were indeed upregulated, whereas the expression of miRNAs (let-7c and let-7f) associated with M2 macrophages were indeed downregulated. To clarify some of the possible related mechanisms, KEGG analysis was performed on the target genes of the different miRNA. The results in Figure 2G showed the greatest correlation with the Wnt signaling pathway, and thus the polarizing mechanism of M1-Exos on macrophages was likely the Wnt signaling diagram. Figures 2H and 2I showed that after M1-Exos treatment, the Wnt signaling pathway of RAW264.7 is inhibited. Therefore, we suspect that the M1-Exos polarized macrophages have the M1 phenotype and the inhibition of the Wnt signaling pathway of macrophages has a great correlation.

$M1_{OVA}$-Exos can effectively inhibit the growth and metastasis of B16-OVA melanoma. As shown in Figures 3 and 5, $M1_{OVA}$-Exos can not only inhibit the growth of tumor, but also inhibit its metastasis to the lungs and prolong the survival time of mice. As shown in Figure 4, immune cells infiltration after treatment was analyzed. After $M1_{OVA}$-Exos treatment, macrophages in mouse tumor tissues were polarized to the greatest extent into M1 type macrophages, which could effectively infiltrate $CD4^+$ T cells, $CD8^+$ T cells, and NK cells. After treatment with $M1_{OVA}$-Exos, the serum of mice was rich in higher levels of pro-inflammatory cytokines (IL-6, IL-12, TNF-α, and IFN-γ), whereas the level of IL-10 was downregulated, and the serum of mice in the $M1_{OVA}$-Exos group had higher levels of OVA antibodies. All these results indicated that M1ova-Exos by polarizing TAM conversion to M1 cells could contribute to changing the microenvironment from highly immunosuppressive to less immunosuppressive type.

In summary, we have constructed an M1-like macrophage exosomal tumor vaccine carrying OVA antigen that can enhance the immunotherapy efficiency of tumor vaccines by polarizing TAMs into M1 macrophages. First, we extracted primary macrophages and polarized them with LPS into M1 macrophages. Then OVA antigens including Exos were isolated. $M1_{OVA}$-Exos exhibited excellent biocompatibility and the ability to polarize macrophages into the M1 type. $M1_{OVA}$-Exos could alleviate the immunosuppressive effect of the TME by polarizing TAMs as immune-support M1 macrophages *in vivo*. In addition, $M1_{OVA}$-Exos could cross-present antigens to T cells to promote the proliferation and activation of T cells to kill tumor cells. $M1_{OVA}$-Exos effectively enhanced the immunotherapy effect of tumor vaccines through the transformation of TAMs, which then inhibited tumor growth and metastasis. However, OVA is not a bona fide tumor antigen. When the study theory was applied to the clinic, the antigen can be extracted from tumor tissue of patients and then combined with M1-Exo for treatment. Therefore, our exosome vaccine provides a new idea for clinical antitumor therapy.

Limitations of the study

The study is limited by using only a single tumor model and the model antigen of OVA. The effects of immunogenic OVA are relatively modest and do not necessarily produce the same therapeutic effect if tested/extrapolated to more authentic antigens. The results of this study are only a basic study on exosome-polarized type M2 macrophages to improve the microenvironment of tumor immunosuppression and thus

enhance the effect of immunotherapy. Because of the complexity of tumor microenvironment and tumor immunity, it is still a long way before clinical application. The next step we will continue to investigate is on its specific polarization mechanism, for example, how the Wnt pathway is affected. In addition, we will further use patient tumor specimens to construct a patient-derived xenografts (PDX) model for further analysis.

STAR★METHODS

Detailed methods are provided in the online version of this paper and include the following:

- KEY RESOURCES TABLE
- RESOURCE AVAILABILITY
  - Lead contact
  - Materials availability
  - Data and code availability
- EXPERIMENTAL MODEL AND SUBJECT DETAILS
  - Primary cell cultures
  - Cell lines
  - Animals
- METHOD DETAILS
  - The preparation of M1-like macrophages carrying OVA
  - The isolation and characterization of $M1_{OVA}$-Exos
  - The uptake of $M1_{OVA}$-Exos by RAW264.7
  - $M1_{OVA}$-Exos polarizes RAW264.7 to M1-like macrophages *in vitro*
  - The mechanism by which M1-Exos polarizes macrophages
  - $M1_{OVA}$-Exos enhances the antigen presentation ability of RAW264.7
  - $M1_{OVA}$-Exos activates T cells *in vitro*
  - FCM analysis
  - Western blot
  - Animal treatments and antitumor effect
  - H&E and TUNEL assay
  - Analysis of immune cells from tumor tissues
  - Detection of cytokines in serum
  - $M1_{OVA}$-Exos inhibits lung metastasis
- QUANTIFICATION AND STATISTICAL ANALYSIS

SUPPLEMENTAL INFORMATION

Supplemental information can be found online at https://doi.org/10.1016/j.isci.2021.103639.

ACKNOWLEDGMENTS

This work was supported by National Natural Science Foundation of China key projects (32030060), NSFC international collaboration key project (51861135103), National Key Research and Development Program of China (2018YFE0117800), NSFC (21977024, 21601046 and 31971304), Beijing-Tianjin-Hebei Basic Research Cooperation Project (19JCZDJC64100), Cross-Disciplinary Project of Hebei University (DXK201916). Science Fund for Creative Research Groups of Nature Science Foundation of Hebei Province (B2021201038). One Hundred Talent Project of Hebei Province (E2018100002). The graphical abstract was created by BioRender.com.

AUTHOR CONTRIBUTIONS

H.L., X.L., and Z.L., designed the project. J.Z., and X.Y., contributed to the experimental design of the study. F.L. performed most of the experiments and the data analysis. G.Z., E.Z., H.Y., and X.Z., contributed to performing parts of experiments. H.L., X.L., and Z.L., edited the manuscript. All authors read and approved the final manuscript.

DECLARATION OF INTEREST

The authors declare no competing interests.

Received: July 31, 2021
Revised: October 21, 2021
Accepted: December 13, 2021
Published: January 21, 2022

REFERENCES

Chen, D., Xie, J., Fiskesund, R., Dong, W., Liang, X., Lv, J., Jin, X., Liu, J., Mo, S., Zhang, T., et al. (2018). Chloroquine modulates antitumor immune response by resetting tumor-associated macrophages toward M1 phenotype. Nat. Commun. *9*, 873. https://doi.org/10.1038/s41467-018-03225-9.

Cheng, L., Wang, Y., and Huang, L. (2017). Exosomes from M1-polarized macrophages potentiate the cancer vaccine by creating a pro-inflammatory microenvironment in the lymph node. Mol. Ther. *25*, 1665–1675. https://doi.org/10.1016/j.ymthe.2017.02.007.

Colombo, M., Raposo, G., and Théry, C. (2014). Biogenesis, secretion, and intercellular interactions of exosomes and other extracellular vesicles. Annu. Rev. Cell Dev. Biol. *30*, 255–289. https://doi.org/10.1146/annurev-cellbio-101512-122326.

Couzin-Frankel, J. (2013). Cancer immunotherapy. Science *342*, 1432–1433. https://doi.org/10.1126/science.342.6165.1432.

Davis, R.J., Waes, C.V., and Allen, C.T. (2016). Overcoming barriers to effective immunotherapy: MDSCs, TAMs, and Tregs as mediators of the immunosuppressive microenvironment in head and neck cancer. Oral Oncol. *58*, 59–70. https://doi.org/10.1016/j.oraloncology.2016.05.002.

Duan, F., Feng, X., Yang, X., Sun, W., Jin, Y., Liu, H., Ge, K., Li, Z., and Zhang, J. (2017). A simple and powerful co-delivery system based on ph-responsive metal-organic frameworks for enhanced cancer immunotherapy. Biomaterials *122*, 23–33. https://doi.org/10.1016/j.biomaterials.2017.01.017.

Fang, B., Chen, X., Wu, M., Kong, H., Chu, G., Zhou, Z., Zhang, C., and Chen, B. (2018). Luteolin inhibits angiogenesis of the M2-like TAMs via the downregulation of hypoxia inducible factor-1α and the STAT3 signalling pathway under hypoxia. Mol. Med. Rep. *18*, 2914–2922. https://doi.org/10.3892/mmr.2018.9250.

Gao, S., Yang, D.J., Fang, Y., Lin, X.J., Jin, X.C., Wang, Q., Wang, X.Y., Ke, L.Y., and Shi, K. (2019). Engineering nanoparticles for targeted remodeling of the tumor microenvironment to improve cancer immunotherapy. Theranostics *9*, 126–151. https://doi.org/10.7150/thno.29431.

Goldman, N., Valiuskyte, K., Londregan, J., Swider, A., Somerville, J., and Riggs, J.E. (2017). Macrophage regulation of B cell proliferation. Cell. Immunol. *314*, 54–62. https://doi.org/10.1016/j.cellimm.2017.02.002.

Guilliams, M., and Svedberg, F.R. (2021). Does tissue imprinting restrict macrophage plasticity? Nat. Immunol. *22*, 118–127. https://doi.org/10.1038/s41590-020-00849-2.

Hanahan, D., and Weinberg, R.A. (2011). Hallmarks of cancer: the next generation. Cell *144*, 646–674. https://doi.org/10.1016/j.cell.2011.02.013.

Jeppesen, D.K., Fenix, A.M., Franklin, J.L., Higginbotham, J.N., Zhang, Q., Zimmerman, L.J., Liebler, D.C., Ping, J., Liu, Q., Evans, R., et al. (2019). Reassessment of exosome composition. Cell *177*, 428–445. https://doi.org/10.1016/j.cell.2019.02.029.

Kalluri, R. (2016). The biology and function of exosomes in cancer. J. Clin. Invest. *126*, 1208–1215. https://doi.org/10.1172/JCI81135.

Kalluri, R., and Lebleu, V.S. (2020). The biology, function, and biomedical applications of exosomes. Science *367*, eaau6977. https://doi.org/10.1126/science.aau6977.

Ke, W., and Afonin, K.A. (2021). Exosomes as natural delivery carriers for programmable therapeutic nucleic acid nanoparticles (NANPs). Adv. Drug Deliver. Rev. https://doi.org/10.1016/j.addr.2021.113835.

Lan, J., Sun, L., Xu, F., Liu, L., Hu, F., Song, D., Hou, Z., Wu, W., Luo, X., Wang, J., et al. (2019). M2 macrophage-derived exosomes promote cell migration and invasion in colon cancer. Cancer Res. *79*, 146–158. https://doi.org/10.1158/0008-5472.CAN-18-0014.

Li, L., Zhang, L.B., and Knez, M. (2016). Comparison of two endogenous delivery agents in cancer therapy: exosomes and ferritin. Pharmacol. Res. *110*, 1–9. https://doi.org/10.1016/j.phrs.2016.05.006.

Li, Y.Y., Zhang, Y.T., Li, Z., Zhou, K., and Feng, N.P. (2019). Exosomes as carriers for antitumor therapy. ACS Biomater. Sci. Eng. *5*, 4870–4881. https://doi.org/10.1021/acsbiomaterials.9b00417.

Lei, X., Lei, Y., Li, J.K., Du, W.X., Li, R.G., Yang, J., Li, J., Li, F., and Tan, H.B. (2020). Immune cells within the tumor microenvironment: biological functions and roles in cancer immunotherapy. Cancer Lett. *470*, 126–133. https://doi.org/10.1016/j.canlet.2019.11.009.

Leick, K.M., Pinczewski, J., Mauldin, I.S., Young, S.J., and Slingluff, C.L. (2019). Patterns of immune-cell infiltration in murine models of melanoma: roles of antigen and tissue site in creating inflamed tumors. Cancer Immunol. Immunother. *68*, 1121–1132. https://doi.org/10.1007/s00262-019-02345-5.

Liu, C.Y., and Su, C.Q. (2019). Design strategies and application progress of therapeutic exosomes. Theranostics *9*, 1015–1028. https://doi.org/10.7150/thno.30853.

Locati, M., Curtale, G., and Mantovani, A. (2019). Diversity, mechanisms, and significance of macrophage plasticity. Ann. Rev. Paleopathol. Mech. Dis. *15*, 1–25. https://doi.org/10.1146/annurev-pathmechdis-012418-012718.

Lopez-Yrigoyen, M., Cassetta, L., and Pollard, J.W. (2020). Macrophage targeting in cancer. Ann. N. Y. Acad. Sci. *2020*, 1–24. https://doi.org/10.1111/nyas.14377.

Lv, J., Chen, F.K., Liu, C., Liu, P.J., and Deng, Z.Y. (2020). Zoledronic acid inhibits thyroid cancer stemness and metastasis by repressing M2-like tumor-associated macrophages induced wnt/β-catenin pathway. Life Sci. *256*, 117925. https://doi.org/10.1016/j.lfs.2020.117925.

Nie, W.D., Wu, G.H., Zhang, J.F., Huang, L.L., Ding, J.J., Jiang, A.Q., Zhang, Y.H., Liu, Y.H., Li, J.C., Pu, K.Y., et al. (2020). Responsive exosome nano-bioconjugates for synergistic cancer therapy. Angew. Chem. Int. Ed. *59*. https://doi.org/10.1002/anie.201912524.

Pegtel, D.M., and Gould, S.J. (2019). Exosomes. Annu. Rev. Biochem. *88*, 487–514. https://doi.org/10.1146/annurev-biochem-013118-111902.

Rodell, C.B., Arlauckas, S.P., Cuccarese, M.F., Garris, C.S., Li, R., Ahmed, M.S., Kohler, R.H., Pittet, M.J., and Weissleder, R. (2018). Tlr7/8-agonist-loadednanoparticles promote the polarization of tumour -associatedmacrophages to enhance cancer immunotherapy. Nat. Biomed. Eng. *2*, 578–588. https://doi.org/10.1038/s41551-018-0236-8.

Sha, H., Zhang, D., Zhang, Y., Wen, Y., and Wang, Y. (2017). ATF3 promotes migration and M1/M2 polarization of macrophages by activating tenascin-C via Wnt/β-catenin pathway. Mol. Med. Rep. *16*, 3641–3647. https://doi.org/10.3892/mmr.2017.6992.

Singh, Y., Pawar, V.K., Meher, J.G., Raval, K., Kumar, A., Shrivastava, R., Bhadauriab, S., and Chourasia, M.K. (2017). Targeting tumor associated macrophages (TAMs) via nanocarriers. J. Control Release *254*, 92–106. https://doi.org/10.1016/j.jconrel.2017.03.395.

Trams, E.G., Lauter, C.J., Salem, J.N., and Heine, U. (1981). Exfoliation of membrane ecto-enzymes in the form of micro-vesicles. BBA-Biomembr. *645*, 63–70. https://doi.org/10.1016/0005-2736(81)90512-5.

Vitale, I., Manic, G., Coussens, L.M., Kroemer, G., and Galluzzi, L. (2019). Macrophages and metabolism in the tumor microenvironment. Cell Metab. *30*, 36–50. https://doi.org/10.1016/j.cmet.2019.06.001.

Wang, Y., Lin, Y.X., Qiao, S.L., An, H.W., Ma, Y., Qiao, Z.Y., Rajapaksha, R.P.Y.J., and Wang, H. (2017). Polymeric nanoparticles promote macrophage reversal from m2 to m1 phenotypes in the tumor microenvironment. Biomaterials *112*, 153–163. https://doi.org/10.1016/j.biomaterials.2016.09.034.

Wang, P.P., Wang, H.H., Huang, Q.Q., Peng, C., Yao, L., Chen, H., Qiu, Z., Wu, Y.F., Wang, L., and Chen, W.D. (2019). Exosomes from M1-polarized

macrophages enhance paclitaxel antitumor activity by activating macrophages-mediated inflammation. Theranostics *9*, 1714–1727. https://doi.org/10.7150/thno.30716.

Xu, J., Wang, H., Xu, L., Yu, C., Wang, C., Han, X., Dong, Z., Chang, H., Peng, R., Cheng, Y., and Liu, Z. (2019). Nanovaccine based on a protein-delivering dendrimer for effective antigen cross-presentation and cancer immunotherapy-sciencedirect. Biomaterials *207*, 1–9. https://doi.org/10.1016/j.biomaterials.2019.03.037.

Yang, Q., Guo, N.N., Zhou, Y., Chen, J.J., Wei, Q.C., and Han, M. (2020). The role of tumor-associated macrophages (TAMs) in tumor progression and relevant advance in targeted therapy. Acta Pharm. Sin. B *10*, 2156–2170. https://doi.org/10.1016/j.apsb.2020.04.004.

Zanganeh, S., Hutter, G., Spitler, R., Lenkov, O., Mahmoudi, M., Shaw, A., Pajarinen, J.S., Nejadnik, H., Goodman, S., Moseley, M., et al. (2016). Iron oxide nanoparticles inhibit tumour growth by inducing pro-inflammatory macrophage polarization in tumour tissues. Nat. Nanotechnol. *11*, 986–994. https://doi.org/10.1038/NNANO.2016.168.

Zhang, J.Y., Shi, Z.P., Xu, X., Yu, Z.R., and Mi, J. (2019). The influence of microenvironment on tumor immunotherapy. FEBS J. *286*, 4160–4175. https://doi.org/10.1111/febs.15028.

Zhu, L., Sun, H.T., Wang, S., Huang, S.L., Zheng, Y., Wang, C.Q., Hu, B.Y., Qin, W., Zou, T.T., Fu, Y., et al. (2020). Isolation and characterization of exosomes for cancer research. J. Hematol. Oncol. *13*, 1–24. https://doi.org/10.1186/s13045-020-00987-y.

STAR★METHODS

KEY RESOURCES TABLE

REAGENT or RESOURCE	SOURCE	IDENTIFIER
Antibodies		
APC anti-mouse F4/80	Biolegend	Cat#123115; RRID: AB_893493
AF488 anti-mouse CD68	Biolegend	Cat#137011; RRID: AB_2074847
PE anti-mouse CD80	Biolegend	Cat#bs-1479R-PE; RRID: AB_313128
FITC anti-mouse CD206	Biolegend	Cat#bs-23178R-FITC; RRID: AB_10900988
Rabbit Anti-iNOS antibody	Bioss	Cat#bs-2072R
Rabbit Anti-Arginase 1 antibody	Bioss	Cat#bs-8585R
Rabbit Anti-CD81 antibody	Bioss	Cat#bsm-51378M
Rabbit Anti-CD63 antibody	Bioss	Cat#bs-23032R
Tsg101 Rabbit Polyclonal antibody	Proteintech	Cat#28283-1-AP; RRID: AB_2881104
Rabbit Anti-Beta catenin/AF594	Bioss	Cat#bs-1165R-AF594
Rabbit Anti-Beta catenin Polyclonal Antibody	Bioss	Cat#bs-1165R; RRID: AB_10855681
Rabbit Anti-C-Myc Polyclonal Antibody	Bioss	Cat#bs-24507R
Rabbit Anti-Cyclin D1 Polyclonal Antibody	Bioss	Cat#bs-20596R
SIINFEKL peptide bound to H-2Kb Monoclonal Antibody, PE	Thermo Fisher Scientific	Cat#12-5743-82; RRID: AB_925774
PE anti-mouse CD8a	Biolegend	Cat#162303; RRID: AB_2894434
PE anti-mouse CD4	Biolegend	Cat#100407; RRID: AB_312692
Chemicals, peptides, and recombinant proteins		
Lipopolysaccharid (LPS)	Solarbio	Cat#L8880
OVA-FITC conjugated	Bioss	Cat#bs-0283P-FITC
Critical commercial assays		
ECL Western Blotting Substrate Kit	abcam	Cat#ab65623
Mouse IL-10 ELISA KIT	Bioss	Cat#bsk12007
Mouse IL-6 ELISA KIT	Bioss	Cat#bsk12004
Mouse IL-12 ELISA KIT	Bioss	Cat#bsk12020
Mouse IFN-γ ELISA KIT	Bioss	Cat#bsk12001
Mouse TNF-α ELISA KIT	Bioss	Cat#bsk12002
Deposited data		
RNAseq	This paper	GEO: GSE190619
Experimental models: Cell lines		
B16-OVA	Shanghai Institute of Biochemistry and Cell Biology, Shanghai Science Research Center, Chinese Academy of Sciences, China	N/A
RAW264.7	Peking Union Cell Resource Center	N/A
Jurkat, Clone E6-1	Procell Life Science & Technology Co., Ltd	Cat#CL-0129
Experimental models: Organisms/strains		
Mouse: C57BL/6	Vital River Experimental Animal Technology Co., Ltd	N/A
Software and algorithms		
GraphPad Prism8	GraphPad	https://www.graphpad.com/

RESOURCE AVAILABILITY

Lead contact

Further information and requests for resources and reagents should be directed to and will be fulfilled by the lead contact, Xing-jie Liang (liangxj@nanoctr.cn).

Materials availability

This study did not generate new unique reagents.

Data and code availability

The data reported in this study is available upon request from the lead contact, Xing-jie Liang (liangxj@nanoctr.cn). The RNA sequence datasets during this study are available at the Gene Expression Omnibus (GEO) site with accession number GEO: GSE190619.

This paper does not report original code.

Any additional information required to reanalyze the data reported in this paper is available from the lead contact upon request.

EXPERIMENTAL MODEL AND SUBJECT DETAILS

Primary cell cultures

C57BL/6 mice (6-10 weeks old) were starved for 8 h before being sacrificed. These mice were immersed and disinfected with 75% alcohol, and the following operations were performed on a super clean bench. All items used on the super clean bench were clean and sterile. First, the mice were fixed to a foam board, after which tweezers were used to lift their abdominal fur, which was cut with scissors, taking care not to cut the endothelium. This was followed by lifting the endothelium with tweezers and making a small incision with scissors, after which forceps were used to open the endothelial wound. Then, a cold DMEM complete medium was poured into the abdominal cavity, and a gentle press was applied to the abdomen for an adequate lavage. Finally, the abdominal lavage fluid was collected. After repeating the lavage several times, the collected lavage fluid was centrifuged (1000 rpm, 5 min), the supernatant was then removed, and the cells were resuspended in a DMEM complete medium for culturing. After the cells adhered, the non-adherent cells were washed away with PBS. The extracted cells were cultured at 37°C, 5% CO_2 and humidity at saturation. The identification of macrophages was performed by ink phagocytosis experiments, confocal laser scanning microscopy (CLSM) and flow cytometry (FCM).

Cell lines

B16-OVA cells were kindly provided by Prof. Chenqi Xu (Shanghai Institute of Biochemistry and Cell Biology, Shanghai Science Research Center, Chinese Academy of Sciences, China). RAW264.7 cells were purchased from Peking Union Cell Resource Center. Jurkat, Clone E6-1 (Procell CL-0129) were kindly provided by Procell Life Science & Technology Co., Ltd.

Animals

Female C57BL/6 mice (5 weeks old) were purchased from Vital River Experimental Animal Technology Co., Ltd. All animal experiments were performed strictly in accordance with the regulations of the Experimental Animal Ethics Committee of Hebei University.

METHOD DETAILS

The preparation of M1-like macrophages carrying OVA

The primary macrophages were incubated with 100 ng/mL LPS for 12 h and polarized into the M1 phenotype. The identification of the macrophage phenotype was carried out by Western Blot (WB), CLSM and FCM. Next, the M1-like macrophages were incubated for 24 h with 0.1 mg/mL OVA. To facilitate the observation of OVA antigen uptake by the macrophages, fluorescein isothiocyanate (FITC)-labeled OVA (OVA-FITC) was used instead of naked OVA. Then, the uptake of OVA by M1-like macrophages was verified by FCM and CLSM.

The isolation and characterization of $M1_{OVA}$-Exos

M1-like macrophages carrying OVA were cultured for two days, after which the cell culture supernatant was collected and centrifuged at 4500×g in a 100-kD ultrafiltration centrifuge tube at 4°C to concentrate Exos and remove small particles in the culture supernatant. Then, the supernatant was centrifuged at 10,000×g at 4°C for 45 min to remove larger vesicles. The obtained supernatant was ultracentrifuged at 100,000×g at 4°C for 70 min. The remainder was resuspended in the centrifuge tube with 10 mL of pre-cooled PBS and then ultracentrifuged once again at 100,000×g for 70 min at 4°C. The supernatant was subsequently removed, and the remainder was resuspended in the centrifuge tube again with 100 μL of pre-cooled PBS to obtain $M1_{OVA}$-Exos. The same method was used to collect the culture supernatant of M0-type macrophages and M1-type macrophages to obtain M0-Exos and M1-Exos, respectively. Exos prepared in this way can be stored for a long time at -80°C.

Following this, we used transmission electron microscopy (TEM), dynamic light scattering (DLS) and nanoparticle tracking analysis (NTA) to characterize the morphology, particle size distribution, particle density and Zeta potential of $M1_{OVA}$-Exos. In addition, WB and FCM were used to analyze the marker proteins of Exos.

The uptake of $M1_{OVA}$-Exos by RAW264.7

$M1_{OVA}$-Exos was labeled with DiO and incubated with RAW264.7 and B16-OVA, respectively. The uptake of RAW264.7 and B16-OVA in Exos were observed by CLSM and FCM.

$M1_{OVA}$-Exos polarizes RAW264.7 to M1-like macrophages *in vitro*

CLSM was used to observe the phenotype of the macrophages. RAW264.7 cells were seeded into a small confocal culture dish at a concentration of 1×10^5 cells/mL. After overnight adhesion, PBS, OVA, M0-Exos, M1-Exos and $M1_{OVA}$-Exos were incubated with RAW264.7. The cells were stained with CD80/PE and CD206/FITC, and the nuclei were labeled with Hoechst 33342.

The mechanism by which M1-Exos polarizes macrophages

To explore the mechanism by which M1-Exos polarizes macrophages of the M1 phenotype, the micRNA of M0-Exos and M1-Exos were extracted from different samples and mixed together, and this micRNA was sequenced. The target genes of different strands of micRNA were found, and Kyoto Encyclopedia of Genes and Genomes (KEGG) analysis was performed on them to explore the relevant signaling pathways.

$M1_{OVA}$-Exos enhances the antigen presentation ability of RAW264.7

The effect of $M1_{OVA}$-Exos on the antigen presentation ability of macrophages was studied by FCM. The RAW264.7 was divided into five groups and treated with PBS, OVA, M0-Exos, M1-Exos and $M1_{OVA}$-Exos, and then it was co-cultured with B16-OVA at a ratio of 1:1. The cells were labeled with SIINFEKL peptide bound to the H-2Kb monoclonal antibody/PE.

$M1_{OVA}$-Exos activates T cells *in vitro*

FCM was used to analyze the activation of T cells into $CD4^+$ T cells and $CD8^+$ T cells by $M1_{OVA}$-Exos. Jurkat (clone E6-1) was divided into five groups and treated with PBS, OVA, M0-Exos, M1-Exos and $M1_{OVA}$-Exos. The treated Jurkat (clone E6-1) cells were incubated with CD8a/PE and CD4/PE.

FCM analysis

The cultured cells were washed with PBS, trypsinized and centrifuged to collect the cells. The cells were incubated with a fluorescently labeled antibody (such as F4/80/APC, CD68/AF488, CD80/PE, CD206/FITC, SIINFEKL/PE, CD4/PE or CD8a/PE) at 37°C for 30 min, centrifuged for cell collection and washed three times with PBS. Finally, they were resuspend in 1 ml of PBS and analyzed via FCM.

Western blot

The cell lysate and protease inhibitor were mixed uniformly at a ratio of 1000:4, and an appropriate amount of the mixed cell lysate was used to lyse the cell or Exos sample on ice for 5 min. The lysed cells or Exos were collected, sonicated and centrifuged at 13,000 rpm for 10 min at 4°C. The supernatant was then collected and stored at -80°C.

An SDS-PAGE gel was prepared, and BCA protein quantification was then conducted on the lysed protein sample, after which the amount of protein loaded per well was 30 μg. The protein sample was mixed with a 5 × bromophenol blue buffer in a 4:1 ratio and then heated at 100°C for 5 min to denature the protein. Under a 60-V constant voltage, the protein sample was concentrated in the stacking gel. When the protein sample ran to the separating gel, the voltage was changed to 80 V. When the protein sample ran to the bottom of the gel, it was treated with a constant current of 0.2 mA at a low temperature for 3 h to transfer the protein to the PVDF membrane. Then, it was blocked with 5% BSA blocking solution at room temperature for 1 h. The appropriate position was then selected according to the Marker, and the antibody was incubated overnight at 4°C. The next day, the sample was placed on a shaker until the temperature returned to room temperature, after which it was washed with membrane washing solution to remove excess antibody. It was incubated with Goat Anti-rabbit IgG/HRP for 1 h at room temperature. Then, the excess antibody was washed off once again. Its color was developed with an ECL kit, and it was photographed with a gel imager.

Animal treatments and antitumor effect

We established B16-OVA mouse models. In brief, B16-OVA cells were digested with trypsin and washed twice with normal saline; then, the cell density was adjusted to 5×10^6 cells/mL. 5-week-old C57BL/6 female mice were used for modeling, and 100 μL of the aforementioned B16-OVA cell suspension was subcutaneously inoculated on the right back side of each mouse (Duan et al., 2017). When their tumor volume was close to 100 mm^3, the animals were randomly divided into 5 groups: PBS group, OVA group, M0-Exos group, M1-Exos group and $M1_{OVA}$-Exos group. Each group contained ten mice. Tumor-bearing mice were injected three times by tail vein injection with PBS, OVA (100 μg per mouse), M0-Exos (10^{10} Exos per mouse), M1-Exos (10^{10} Exos per mouse) and $M1_{OVA}$-Exos (10^{10} Exos per mouse). The mice were sacrificed on the 40th day after the first administration. The tumor-bearing mice were observed, and their survival status was recorded every day. Their tumor volumes and body weights were measured every two days. To observe the biodistribution of $M1_{OVA}$-Exos, $M1_{OVA}$-Exos labeled with DiD dye was intravenously injected into tumor-bearing mice. The mice were imaged and recorded at 2, 4, 8, 12 and 24 hours.

H&E and TUNEL assay

After treatment, all mice were anesthetized and then sacrificed by exsanguination. Their main organs (spleens, lungs, hearts, livers and kidneys) and tumor tissues were separated. Paraffin sections were made. The tissue sections were stained with hematoxylin and eosin (H&E) for pathological analysis. Tumor tissue apoptosis was detected by TUNEL assay.

Analysis of immune cells from tumor tissues

The fresh tumor tissues of each group of mice were crushed by a cell sieve and then dispersed into single cells and diluted with PBS to a cell concentration of 1×10^6 cells/mL. The extracted tumor tissue cells were labeled as CD80/PE, CD206/FITC, CD4/PE and CD8a/PE, and the fluorescence intensity of each group of mice tumor cells were analyzed by FCM. The unlabeled tumor tissue was used as a negative control for comparison. The tumor tissues of each group of mice were analyzed by immunohistochemistry (IHC). The CD80, CD206, CD4, CD8a and CD161 positive cells in the tumor tissue of each group of mice were observed and counted. The tumor tissues of each group of mice were lysed to extract proteins, and the expression changes of iNOs and Arg-1 in each group of tumor tissues were observed by WB.

Detection of cytokines in serum

Blood samples were collected from mice in each group through orbital blood collection. These samples were left to coagulate naturally at room temperature for about 20 min and then centrifuged at 2000 rpm for 5 min. Finally, the supernatant was collected as a serum sample. ELISA kits of IL-6, IL-10, IL-12, IFN-γ and TNF-α were used to determine the cytokine content in different groups' serum.

$M1_{OVA}$-Exos inhibits lung metastasis

For inoculation, a B16-OVA tumor model was established in 5-week-old C57BL/6 female mice. When the tumor volume grew to about 100 mm^3, the mice were randomly divided into 5 groups (PBS group, OVA group, M0-Exos group, M1-Exos group and $M1_{OVA}$-Exos group, with eight mice per group), and these mice were treated accordingly. After one week, B16-OVA cells were injected through the tail vein to simulate the circulation of tumor cells (CTCs).

The survival of the mice was recorded during treatment. On the 20th day after treatment, the mice were sacrificed, and their lung tissues were taken to observe whether there were lung nodules, which were then counted. Lung tissues were analyzed by H&E staining, and $CD4^+$ T cell and $CD8^+$ T cell infiltration of the lung tissue was checked by IHC.

QUANTIFICATION AND STATISTICAL ANALYSIS

The data were presented as mean ± standard deviation (SD). Significance differences between groups were determined by "Student-Newman-Keuls Multiple Comparisons Test" (ANOVA), and $P < 0.05$ was considered as the statistical significance.